Polarizabilities and photoionization cross sections of OH and HF

L. Veseth
Department of Physics, University of Oslo, 0316 Oslo 3, Norway

H. P. Kelly
Department of Physics, University of Virginia, Charlottesville, Virginia 22901
(Received 21 August 1991)

Polarizabilities and photoionization cross sections are computed for the hydrides OH and HF. Finite basis sets are used, with no explicit recourse to continuum orbitals, and single-center expansions are avoided. The present method is based on an integral equation (dispersion relation) that relates the real polarizability on the imaginary frequency axis to the photoionization cross section. Many-body perturbation theory is used to compute the polarizabilities, and the perturbation expansion, which includes a total of 68 distinct diagrams to second order in the Coulomb interaction, is believed to contain all significant terms to that order. Thus there is a comprehensive inclusion of correlation effects, contrary to most molecular photoionization computations presented so far. The present results are compared with those of other computations, and with experiment in the case of HF.

PACS number(s): 32.80.Fb, 33.80.Eh

I. INTRODUCTION

The problem of computing atomic photoionization cross sections continues to pose many challenges for theorists, even after about 20 years of active research in the field. Various methods have been derived to handle this problem, but a common feature of the most sophisticated atomic techniques is that numerical methods are used and that explicit wave functions describing the outgoing unbound electron are sought [1–3]. Besides the problem of obtaining accurate continuum orbitals, the challenges in photoionization computations are posed by many-body effects, which are particularly prominent in this field of atomic physics. A reliable calculation of photoionization cross sections requires a rather thorough inclusion of correlation effects in the initial as well as the final electronic state of the system.

Compared with the high activity in atomic photoionization, the field of molecular photoionization has so far been rather dormant. The reason for this low activity is probably that the sophisticated atomic techniques are not readily applicable to molecules. A main problem is the rather insurmountable difficulties involved in constructing continuum orbitals for multicenter systems. Furthermore, computations on molecules have to be based on finite basis sets, and techniques that are quite different from the numerical atomic methods will generally be required.

Atomic methods have nonetheless been of value for light diatomic hydrides like CH, OH, and HF. For such systems continuum orbitals have been obtained from single-center expansions, normally about the heavy nucleus [4–7]. The effect of the H atom is then in the next step handled by perturbation theory. Various variational techniques are commonly used to derive the continuum orbitals in the molecular case [6–9]. However, the molecular single-center expansion computations are so far on the Hartree-Fock level of accuracy.

A few methods to compute atomic and molecular photoionization cross sections by use of basis sets have been developed so far. The Stieltjes method [10–12] represents an algebraic approach to the problem that makes no explicit recourse to continuum orbitals. The continuum of the system is represented by a series of pseudostates obtained from general techniques in quantum chemistry. Several molecular computations, which tend to be quite successful, have been carried out according to the Stieltjes method [12–15]. Although the Stieltjes method should be capable of including many-body effects, the results presented so far seem to be on the independent-particle level of accuracy.

Another class of methods using finite basis sets is the technique of analytic continuation [16–19]. Successful applications of those methods, however, are so far mostly limited to very small atomic and molecular systems. The most promising of the analytic continuation methods seems to be the complex-basis-functions technique, which has been used to obtain partial cross sections for N_2 [19].

The present work is based on another algebraic approach with no explicit recourse to continuum orbitals, and the method does not in any essential way discriminate between atomic and molecular systems. A more detailed description of the present approach has been given in a preceding paper by one of the present authors [20] (hereafter referred to as I). As all methods to compute photoionization cross sections for many-body systems will be based on approximations, it is of general interest to have various approaches that emphasize different aspects of the theory. The strength of the present method should be its potential for predicting accurate total molecular photoionization cross sections over a wide range of frequencies. The method is, in addition, conceptually simple; the technical problems are limited to computing the (real) polarizability on the imaginary frequen-

 ©1992 The American Physical Society

cy axis where the polarizability has no poles. The deficiency of the present method is certainly that, at least in its current state of development, it does not yield partial cross sections or reproduce narrow resonances. This is, however, a general problem with finite-basis-set methods.

The diatomic hydrides OH and HF have been chosen as molecular test cases. Although the experimental data on these systems are rather sparse, there are other extensive theoretical results for comparison. Work is at present in progress for molecules like CO, N_2, and NO.

II. THEORY

A. The dynamic polarizability of diatomic molecules

The dynamic polarizability represents the linear response of an atomic or molecular system to an external field and is defined by the equation

$$\mathbf{p}=\alpha(\omega)\mathbf{F} , \tag{1}$$

where $\mathbf{p}$ is the electric dipole moment and $\mathbf{F}$ is the applied external field. The external field will be assumed to be of the form $F\cos(\omega t)$, directed along the space-fixed Z axis, and the interaction with the external field adds a time-dependent perturbation given by

$$V_{\rm ex}(t)=F\cos(\omega t)\sum_{i=1}^{N} Z_i=\tfrac{1}{2}(e^{i\omega t}+e^{-i\omega t})Fd_Z . \tag{2}$$

For a freely rotating diatomic molecule the observable polarizability will be an average over the three perpendicular molecule-fixed directions [21] x, y, and z, i.e.,

$$\begin{aligned}\alpha(\omega)&=\tfrac{1}{3}[\alpha_x(\omega)+\alpha_y(\omega)+\alpha_z(\omega)]\\&=\tfrac{1}{3}[2\alpha_\perp(\omega)+\alpha_\parallel(\omega)] .\end{aligned} \tag{3}$$

Disregarding vibrational motion of the molecule, the dynamic electronic polarizability of a diatomic molecule in an electronic state $|\Psi_n\rangle$ is then given by [22]

$$\begin{aligned}\alpha_\parallel(\omega)&=\alpha_z(\omega)\\&=-\sum_{k\ (\neq n)}|\langle\Psi_k|d_z|\Psi_n\rangle|^2\\&\quad\times\left[\frac{1}{E_n-E_k-\omega}+\frac{1}{E_n-E_k+\omega}\right] .\end{aligned} \tag{4}$$

The expression for $\alpha_\perp(\omega)=\alpha_x(\omega)=\alpha_y(\omega)$ is similar to that for $\alpha_\parallel(\omega)$ of Eq. (4), except that the dipole moment d_z along the molecular axis is replaced by d_x or d_y.

In Eq. (4) above the summation is over bound excited electronic states, and an integral over continuum states. Hence, a reliable computation of the polarizability requires an accurate representation of bound as well as continuum states of the total zero-field molecular electronic Hamiltonian.

B. Many-body calculation of $\alpha(\omega)$

In the present work the dynamic polarizability $\alpha(\omega)$ will be computed by use of many-body perturbation theory, as discussed in more detail in I. The many-body expression for $\alpha(\omega)$ to be used in the present investigation takes the form

$$\alpha_z(\omega)=-(\langle\Psi_0|d_z|\Psi_1^+\rangle+\langle\Psi_0|d_z|\Psi_1^-\rangle)/\langle\Psi_0|\Psi_0\rangle , \tag{5}$$

where $|\Psi_1^\pm\rangle$ is given by the linked-cluster expansions [23]

$$\begin{aligned}|\Psi_1^\pm\rangle=\sum_L \frac{1}{E_0-H_0\mp\omega}H'\cdots\frac{1}{E_0-H_0\mp\omega}d_z\\\times\cdots\frac{1}{E_0-H_0}H'|\Phi_0\rangle .\end{aligned} \tag{6}$$

The Hamiltonians H_0 and H' of Eq. (6) and the total electronic Hamiltonian H are defined by

$$\begin{aligned}H_0&=\sum_{i=1}^{N}\left[-\tfrac{1}{2}\nabla_i^2-\frac{Z}{r_i}+V_i\right] ,\\H'&=\sum_{i<j=1}^{N}\frac{1}{r_{ij}}-\sum_{i=1}^{N}V_i ,\\H&=H_0+H' .\end{aligned} \tag{7}$$

Only the ground state of the molecule is of current interest, and E_0 of Eq. (6) denotes the lowest eigenvalue of H_0, with corresponding eigenstate $|\Phi_0\rangle$. The linked-cluster expansion of Eq. (6) with no interaction with d_z yields the correct expression for the ground state $|\Psi_0\rangle$ of the total Hamiltonian H of Eq. (7). The expressions for $\alpha_x(\omega)$ or $\alpha_y(\omega)$ are similar to Eq. (5), with d_z replaced by d_x or d_y, respectively.

The partition of the Hamiltonian of Eq. (7) is normally referred to as the model Hamiltonian, or Möller-Plesset Hamiltonian. Doing many-body perturbation theory, it is of great interest to compare the results obtained with different partitionings of the Hamiltonian. Another widely used partitioning of the Hamiltonian is the shifted or Epstein-Nesbet Hamiltonian defined by [24,25]

$$\begin{aligned}\mathcal{H}_0&=\sum_{l=0}|\Phi_l\rangle\langle\Phi_l|H|\Phi_l\rangle\langle\Phi_l| ,\\\mathcal{H}'&=\sum_{k\neq l}\sum_{l=0}|\Phi_k\rangle\langle\Phi_k|H|\Phi_l\rangle\langle\Phi_l| ,\\H&=\mathcal{H}_0+\mathcal{H}' ,\end{aligned} \tag{8}$$

where $\{|\Phi_l\rangle\}$ denotes the complete set of eigenstates of H_0 of Eq. (7). If the linked-cluster expansion of Eq. (6) is based on the partition $H=\mathcal{H}_0+\mathcal{H}'$, the denominators will be shifted, and there will be no diagonal elements in $\mathcal{H}'$ due to the restriction $k\neq l$ in the summation that defines $\mathcal{H}'$. The diagonal elements that are omitted by use of the shifted Hamiltonian are actually included to all orders through the denominator shifts caused by applying $\mathcal{H}_0$ instead of H_0 in the perturbation expansion. In many-body calculations of atomic polarizabilities, it has normally been found that the terms included to all orders by the shifted Hamiltonian are the most important

higher-order corrections [3,23]. Anyway, a significant disparity between the results obtained with the two different partitionings of the Hamiltonian will indicate an insufficient convergency of the perturbation expansion.

C. The choice of single-particle potentials

A successful many-body expansion requires a careful selection of the single-particle potentials V_i of Eq. (7). The single-particle potentials yield the important single-particle states $\varphi_m(\mathbf{r}_i)$ from the Schrödinger equation

$$\left[-\tfrac{1}{2}\nabla_i^2-\frac{Z}{r_i}+V_i\right]\varphi_n(\mathbf{r}_i)=\varepsilon_n\varphi_n(\mathbf{r}_i)\ . \tag{9}$$

In the present investigation the single-particle states will be represented by analytic expansions in terms of a finite set of known basis functions. This means that the continuum is described by a finite set of virtual orbitals. The Hartree-Fock potentials V_{HF} are an obvious choice for the potentials V_i. However, that choice leads to excited single-particle states that are rather unphysical, as they are obtained in the field of a neutral system (V^N type of potential). The great benefit of the Hartree-Fock potentials is an extensive cancellation of terms in the perturbation expansion for closed-shell systems, and even for open-shell systems the cancellation will normally be very close. In the perturbation expansion the perturbation H' of Eq. (7) will introduce an effective single-particle potential V_{eff} defined by its matrix elements

$$\langle\varphi_k|V_{\mathrm{eff}}|\varphi_l\rangle=\sum_{n=1}^{N}\langle\varphi_k\varphi_n|0|\varphi_l\varphi_n\rangle-\langle\varphi_k|V|\varphi_l\rangle\ , \tag{10}$$

where

$$0=(1-P_{12})\frac{1}{r_{12}}$$

and where P_{12} is the operator that permutes the coordinates of electrons 1 and 2. Now, it is well known from the definition of the Hartree-Fock potential that all the elements of V_{eff} will vanish for a closed-shell system if V_{HF} is inserted for V in Eq. (10). Even for open-shell systems, the contribution from the effective potential of Eq. (10) will normally be quite insignificant when V_{HF} is inserted for V, at least for higher-order terms in the perturbation expansion.

Doing many-body perturbation theory with finite basis sets, great care has to be exercised if the single-particle potentials are removed from the Hartree-Fock potentials. Potentials that might seem quite physical may actually cause the effective potentials of Eq. (10) to blow up, with a consequent disaster for the perturbation expansion.

In the present work a considerable effort will be taken to construct single-particle potentials for the excited states that are more attractive than the Hartree-Fock potentials, and which also lead to significant improvements of the perturbation expansions. This will be achieved by eliminating or at least minimizing the contribution from the first-order terms in H' in the perturbation expansion.

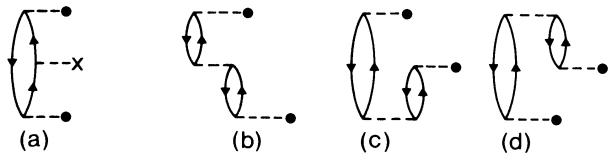

FIG. 1. The four most important first-order diagrams contributing to $\alpha(\omega)$. The heavy dot indicates interaction with the dipole operator, and the cross represents interaction with the effective potential [cf. Eq. (10)].

There are four important first-order diagrams, as shown in Fig. 1. In the static case ($\omega=0$) the contribution $\alpha_z^{(1)}(0)$ from these four most important first-order diagrams takes the form

$$\alpha_z^{(1)}(0)=\sum_{i,j}\left[\langle j|V_{\mathrm{eff}}|i\rangle\sum_p\frac{\langle p|z|j\rangle\langle i|z|p\rangle}{(\varepsilon_p-\varepsilon_j)^2}+\sum_{p,q}\frac{\langle p|z|j\rangle\langle jq|0|pi\rangle\langle i|z|q\rangle}{(\varepsilon_p-\varepsilon_j)(\varepsilon_q-\varepsilon_i)}+\sum_{p,q}\frac{\langle p|z|j\rangle\langle ji|0|pq\rangle\langle i|z|q\rangle}{(\varepsilon_p-\varepsilon_j)(\varepsilon_q-\varepsilon_i)}\right], \tag{11}$$

where 0 is given by Eq. (10).

To obtain Eq. (11), the diagrams of Figs. 1(c) and 1(d) have been added, and the denominators of their mathematical expressions have been reorganized to show their character as effective single excitation diagrams [26]. The problem is now to determine the effective potential V_{eff} of Eq. (10) so that the first-order contribution of Eq. (11) is eliminated, or, in practice, reduced as much as possible. This is achieved through an iterational process, starting with excited orbitals computed for the Hartree-Fock potential. In practice, difficulties may arise, in particular for highly excited orbitals, and some terms in the summations of Eq. (11) will have to be left out, so that the elimination of the first-order contribution will be more or less complete.

The dominant contribution to the correction of the Hartree-Fock potentials for the excited states will normally be provided by the diagram of Fig. 1(b) for $p=q$. Denoting this particular correction of the potential by V_{pp}, its matrix elements will be from Eq. (11):

$$\langle j|V_{pp}|i\rangle=-\left\langle jp\left|\frac{1}{r_{12}}\right|ip\right\rangle+\left\langle jp\left|\frac{1}{r_{12}}\right|pi\right\rangle\ , \tag{12}$$

which is precisely the correction needed to modify the Hartree-Fock potential to a V^{N-1} type of potential. It is, however, interesting to note that a simple correction such as that of Eq. (12) may lead to divergent perturbation expansions. The full correction of Eq. (11) will be found to retain the V^{N-1} character of the potentials, and lead to convergencies that are far better than those of the Hartree-Fock potentials.

The present approach to compute effective potentials is an extension and generalization of the so-called Qian potentials [27] previously used for atoms. The Qian potentials are based on a cancellation of the contributions from

the diagrams of Figs. 1(a) and 1(b) when q and p denote orbitals in the same shell. For light atoms there is often a dominant contribution to the polarizability from a single outer shell, and the Qian procedure is particularly adequate. This is, however, generally not the case for diatomic molecules where several outer shells of different symmetries may yield significant contributions. Hence, the full correction of Eq. (11) is required in the molecular case. Furthermore, the Qian procedure does not eliminate the diagrams of Figs. 1(c) and 1(d), which are often the dominant first-order diagrams.

When the single-particle potentials are worked out, the many-body computation of the molecular polarizabilities proceeds basically as in the atomic case described in I. For the closed-shell atoms treated in I, the perturbation expansions were complete to second order in the Coulomb terms H' or $\mathcal{H}'$. In the present work many more second-order diagrams need to be included since the excited-state potentials are no longer of Hartree-Fock type, and since an open-shell system will be considered. The extra diagrams needed are all the second-order diagrams with one or two interactions with the effective potential of Eq. (10). A considerable effort was made to fully include all the classes of extra diagrams that tend to be of any significance, and a total of 30 diagrams involving V_{eff} were added to the 38 closed-shell second-order diagrams of I.

It is worth noting that the effective potentials as determined from Eq. (11) tend to yield an approximate cancellation of a large number of diagrams that are second-order generalizations of the first-order ones of Fig. 1. The class of diagrams that are nearly cancelled by the effective potential in particular involve the second-order bubble diagrams typical of the random-phase approximation. Hence, with the present choice of potentials, the dominant second-order diagrams will be the true correlation diagrams involving double and triple excitations.

D. Computation of photoionization cross sections

The real dynamic polarizability for imaginary frequencies ($\omega=i\eta$) is, as discussed in I, related to the photoionization cross section $\sigma(\omega)$ through the integral equation

$$\alpha(i\eta)=\frac{c}{2\pi^2}\int_0^\infty \frac{\sigma(\omega)}{\eta^2+\omega^2}d\omega \ . \tag{13}$$

The effective potential discussed in Sec. II C for the static case ($\omega=0$) will be used in the many-body computation of $\alpha(i\eta)$ also for $\eta\neq 0$. This approach will actually turn out to ensure nice convergency properties of the perturbation expansion even for small imaginary frequencies different from zero. Generally, the convergence of the expansion gets less problematic for increasing values of η. To compute polarizabilities for imaginary frequencies is also particularly convenient as there are no poles on the imaginary axis.

The cross section $\sigma(\omega)$ will be derived from the computed values of $\alpha(i\eta)$ by inverting the integral equation (13), as described in I. The inversion is based on expanding $\sigma(\omega)$ in terms of a finite set of N known functions $\psi_n(\omega)$,

$$\sigma(\omega)=\sum_{n=1}^{N} a_n\psi_n(\omega) \ . \tag{14}$$

To make this procedure work, the number of terms N should be kept as low as possible. Hence, some thought has to be given to the selection of the basis functions $\psi_n(\omega)$. Ideally, each of them should have the same basic features as that of the cross section. They should in particular tend to zero for both the limiting cases $\omega\rightarrow 0$ and $\omega\rightarrow\infty$. The present choice is, as in I,

$$\psi_n(\omega)=\omega^3 e^{-k_n\omega} \ . \tag{15}$$

To ensure a linearly independent set of functions, the exponents k_n were chosen according to the relation

$$k_n=k_0C^{n-1} \ , \tag{16}$$

where C is a real constant larger than 1. For a specific atomic or molecular system the constants k_0 and C and the number of terms in Eq. (14) are determined so that an optimal and stable solution of Eq. (13) is attained. The best choice of these parameters will normally require some trial and error. The inversion of Eq. (13) by use of Eqs. (14) and (15) leads to a continuous curve for $\sigma(\omega)$. As the finite basis set yields a representation of bound excited states as well as continuum states, $\alpha(i\eta)$ of Eq. (13) and consequently $\sigma(\omega)$ will contain the contributions from both types of excited states.

The real part of the polarizability $\text{Re}\alpha(\omega)$ on the real axis is obtained from the computed values of $\sigma(\omega)$ and the Kramers-Kronig dispersion relations [28] as

$$\text{Re}\alpha(\omega)=\frac{c}{2\pi^2}\text{P}\int_0^\infty \frac{\sigma(\omega')}{\omega'^2-\omega^2}d\omega' \ . \tag{17}$$

$\text{Re}\alpha(\omega)$ yields information on important optical properties such as the index of refraction and the Verdet constant [29].

III. COMPUTED RESULTS

A. Static polarizabilities of OH and HF

Computed results for the ground states of the closed-shell system HF and the open-shell system OH will be presented in this section. OH and HF have been selected since there are other theoretical studies of these molecules, both on polarizabilities and photoionization cross sections [5,7,14,30,31]. The hydrides also generally retain essential atomic characters, which ensures a reasonable convergence of the many-body expansion. The experimental material available is unfortunately sparse—in particular for OH.

The basis sets used for the present calculations are extensions of the sets of Slater atomic orbitals with optimized exponents published by Cade and Huo [32]. For OH as well as HF, the basis set was extended by a diffuse $2s$, $2p$ and $3d$ orbital on the heavy atom, and a diffuse $1s$ and $2p$ orbital on H. With the orbital exponent in parentheses, the specific extensions are as follows for OH: $\sigma 2s_0(1.0)$, $\sigma 2p_0(0.8)$, $\sigma 1s_H(0.8)$, $\pi 2p_0(0.75)$, $\pi 3d_0(1.1)$, and $\pi 2p_H(1.0)$, and for HF: $\sigma 2s_F(1.0)$, $\sigma 2p_F(0.8)$,

TABLE I. Computed static polarizabilities (in a.u.) for OH and HF. The results were obtained at the equilibrium internuclear separations of $R=1.834$ a.u. and $R=1.733$ a.u. for OH and HF, respectively.

		$\alpha_{\parallel}$		$\alpha_{\perp}$	
Molecule	Potential	Model H	Shifted H	Model H	Shifted H
OH	V^N	8.00	9.25	6.28	6.55
	V^{N-1}	8.46	8.42	7.27	6.58
HF	V^N	5.87	6.71	4.69	5.28
	V^{N-1}	6.26	6.21	5.84	5.33

$\sigma 1s_H(0.9)$, $\pi 2p_F(0.8)$, $\pi 3d_F(1.1)$, and $\pi 2p_H(1.2)$.

In addition, a set of six δ orbitals was included, based on four $3d$ orbitals on the heavy atom and two $3d$ orbitals on H. The δ orbitals were of the even-tempered type, i.e., the exponents were obtained from the relation

$$\zeta_n=\zeta_0 R^{n-1}, \tag{18}$$

with $\zeta_0=0.50$ and $R=1.8$ for O and F, and $\zeta_0=0.75$ and $R=2.0$ for H. Hence, the present basis sets consist of 19 σ orbitals, 11 π orbitals, and 6 δ orbitals. A few tests were also made with a slightly larger basis set (more diffuse orbitals). The results obtained did not, however, deviate from those of the present basis in any significant way. Even the inclusion of a few ϕ orbitals did not lead to significant changes in the computed results.

Computed values of the static polarizabilities ($\omega=0$) are given in Table I for OH and HF. The results are based on a perturbation expansion which is believed to be fairly complete to second order in H' or $\mathcal{H}'$ [cf. Eqs. (7) and (8)], as discussed in Sec. II C. Since there will be a rapid increase in the rate of convergence of the expansion with increasing (imaginary) frequency (cf. Tables II and III), the static case represents the biggest computational challenge. In Table I computed results are given for both the partitioning of the Hamiltonian of Eq. (7) (model Hamiltonian) and that of Eq. (8) (shifted Hamiltonian). Computations were also carried out for two different excited-state potentials. The V^N potential denotes the standard Hartree-Fock potential, whereas V^{N-1} represents the effective potential based on eliminating or minimizing the first-order contributions from the diagrams of Fig. 1 [cf. Eq. (11)].

A striking feature of Table I is the rather large disparity between the values of $\alpha_{\parallel}=\alpha_z$ obtained for the two partitionings of the Hamiltonian with the V^N potential. This disparity is in both cases almost completely removed by the V^{N-1} potential, a result which should give considerable confidence in this potential.

For the perpendicular component $\alpha_{\perp}=\alpha_x=\alpha_y$, the characteristic feature is the high stability of the computed values for the shifted Hamiltonian with regard to changes in the potential. It is also noteworthy that the values of $\alpha_{\perp}$ computed with the shifted Hamiltonian are intermediate between the extremal ones obtained with the model Hamiltonian. Hence, an important conclusion to be made from Table I is that the shifted Hamiltonian with the V^{N-1} potential clearly gives the most reliable results for the static polarizability of OH as well as HF.

TABLE II. Computed values (in a.u.) of $\alpha_{\parallel}(i\eta)$ (upper half of the Table) and $\alpha_{\perp}(i\eta)$ (lower half) for OH. The first and second entries for each η value refer to the V^N and V^{N-1} potentials, respectively.

	Model Hamiltonian, order				Shifted Hamiltonian, order			
η	Zero	First	Second	Total	Zero	First	Second	Total
0.00	6.163	0.667	1.173	8.003	8.693	−2.143	2.703	9.253
	7.124	−0.033	1.364	8.455	6.832	0.118	1.469	8.419
0.15	6.025	0.572	1.062	7.659	8.271	−2.010	2.406	8.667
	6.869	−0.088	1.224	8.005	6.601	0.065	1.324	7.990
0.60	4.581	−0.152	0.290	4.719	5.064	−1.066	0.734	4.732
	4.715	−0.397	0.372	4.690	4.583	−0.255	0.419	4.747
2.00	1.493	−0.380	−0.086	1.027	1.230	−0.181	−0.069	0.980
	1.391	−0.292	−0.060	1.039	1.405	−0.288	−0.061	1.056
0.00	5.202	0.083	0.057	5.342	6.284	−1.047	1.126	6.363
	5.801	−0.580	1.233	6.454	6.028	−0.652	1.068	6.444
0.15	4.907	0.356	0.452	5.715	5.971	−0.982	1.217	6.206
	5.385	−0.276	1.746	6.855	5.730	−0.622	1.185	6.293
0.60	3.736	−0.054	0.024	3.706	3.927	−0.682	0.498	3.743
	3.600	−0.277	0.628	3.951	3.785	−0.463	0.453	3.775
2.00	1.330	−0.259	−0.086	0.985	1.121	−0.168	0.039	0.992
	1.135	−0.163	0.014	0.986	1.125	−0.160	0.025	0.990

TABLE III. Computed values (in a.u.) of $\alpha_{\parallel}(i\eta)$ and $\alpha_{\perp}(i\eta)$ for HF. Explanations as for Table II.

	Model Hamiltonian, order				Shifted Hamiltonian, order			
η	Zero	First	Second	Total	Zero	First	Second	Total
0.00	4.712	0.305	0.852	5.869	6.454	−1.70	1.96	6.71
	5.327	−0.106	1.035	6.256	5.485	−0.227	0.953	6.211
0.20	4.570	0.222	0.747	5.539	6.060	−1.56	1.67	6.17
	5.027	−0.134	0.889	5.828	5.229	−0.262	0.828	5.795
0.60	3.723	−0.154	0.298	3.867	4.227	−0.969	0.672	3.930
	3.790	−0.219	0.319	3.890	3.919	−0.377	0.360	3.902
2.00	1.397	−0.326	−0.032	1.039	1.212	−0.197	0.016	1.031
	1.305	−0.195	−0.070	1.040	1.300	−0.249	0.010	1.061
0.00	3.463	0.509	0.715	4.687	4.561	−0.516	1.238	5.283
	3.985	0.015	1.841	5.841	4.159	−0.202	1.371	5.328
0.20	3.369	0.437	0.626	4.432	4.316	−0.514	1.064	4.866
	3.748	0.018	1.565	5.331	3.954	−0.213	1.177	4.918
0.60	2.814	0.100	0.263	3.177	3.193	−0.453	0.491	3.231
	2.781	−0.048	0.737	3.470	2.980	−0.215	0.509	3.274
2.00	1.183	−0.200	−0.015	0.968	1.077	−0.155	0.041	0.963
	1.043	−0.112	0.052	0.983	1.080	−0.140	0.027	0.966

The computation of $\alpha_{\perp}$ for OH is complicated by the fact that the perturbation expansion is hardly convergent for the model Hamiltonian. The reason is the strong interaction (beyond the lowest order) between the nearly degenerate occupied 3σ state and the unoccupied π state (configuration $1\sigma^2 2\sigma^2 3\sigma^3 \pi^3$). The computed values of $\alpha(i\eta)$, however, show good convergence for $\eta=0.10$ a.u. and higher η values, and the values of $\alpha_{\perp}$ of Table I are based on the lowest-order correction for $\eta=0$ and the first- and second-order contributions for $\eta=0.10$ a.u. The convergency problems are far less dramatic for the shifted Hamiltonian.

No experimental value of the static polarizability seems to be available for OH. The multiconfiguration computation of $\alpha_{\parallel}$ by Adamowicz [30] is 7.54 a.u. at the internuclear separation of $R=1.7946$ a.u. This value is significantly lower than those of Table I.

For HF there is an experimental value of 5.60 a.u. for the isotropic polarizability $\alpha=\frac{1}{3}(\alpha_{\parallel}+2\alpha_{\perp})$ [33]. The experimental value is thus in excellent agreement with the (best) present theoretical value of 5.62 a.u. obtained with the shifted Hamiltonian and the V^{N-1} potential. The most extensive computation of the static polarizability of HF seems to be that of Diercksen *et al.* [31]. Their values are $\alpha_{\parallel}=6.50$ a.u. and $\alpha_{\perp}=5.40$ a.u., respectively, based on a coupled Hartree-Fock method, extended with a fourth-order perturbation expansion. The present static polarizabilities obtained with the shifted Hamiltonian and the V^{N-1} potential are thus in good agreement with the sophisticated results of Diercksen *et al.* The experimental values [34] of the anisotropy $\Delta\alpha=\alpha_{\parallel}-\alpha_{\perp}$ of 1.48 ± 0.14 a.u. is, however, in poor agreement with the present results as well as those of Diercksen *et al.*

B. The dynamic polarizability $\alpha(i\eta)$

The present many-body method is also readily applicable to the computation of dynamic polarizabilities for complex frequencies. Values of $\alpha_{\parallel}(i\eta)$ and $\alpha_{\perp}(i\eta)$ were computed at about 25 points in the range $\eta=0.0$ to 12.0 to serve as a basis for the calculation of $\sigma(\omega)$ from Eq. (13). Computed values are given in Tables II and III for a few η values with specification of the individual contributions from the three lowest orders in the perturbation expansion.

The results of Tables II and III clearly show how the V^{N-1} potential was constructed by minimizing the first-order contribution for $\eta=0$. The same feature is also essentially retained for other low η-values. However, $\alpha_{\perp}(0)$ for OH is an exception since in this case there is a strong interaction between the filled 3σ shell and the open π shell that cannot be eliminated by changing the excited-state potentials. This strong interaction also leads to problems with the convergence of the perturbation expansion, in particular for the model Hamiltonian, as discussed in Sec. III A.

As in the static case, there is also for higher η values very good agreement between the α values obtained with the V^{N-1} potential for the two partitionings of the Hamiltonian. For $\alpha_{\perp}$ the shifted partitioning of the Hamiltonian leads to very close agreement between the results for the two potentials. Hence, there is good reason to conclude that the shifted Hamiltonian with the V^{N-1} potential yields the most reliable estimates of the dynamic polarizabilities $\alpha_{\parallel}(i\eta)$ and $\alpha_{\perp}(i\eta)$ for OH as well as HF.

It is also clear from Tables II and III that the rate of convergence of the perturbation expansion generally increases rather fast with increasing η values. For $\eta=0.60$ a.u. and higher, there is seen to be good agreement among the results of the four different computations.

Contributions beyond the lowest order (Hartree-Fock) in the many-body expansion are normally ascribed to correlation effects. However, the results of Tables II and III clearly reveal that the magnitude of the lowest-order term as well as those of the next two orders are heavily dependent on the single-particle potential and the partitioning of the Hamiltonian. Hence, the concept of correlation is certainly not very well defined in many-body cal-

culations of polarizations. A reasonable and more precise definition of correlation could be to identify this effect with the contribution from double, triple, and higher excitations for a potential like the present V^{N-1} potential, which largely eliminates the single excitations. The second-order corrections of Tables II and III are all for the V^{N-1} potential largely due to true double and triple excitations.

In numerical many-body calculations of atomic polarizabilities and photoionization cross sections, the triple excitations are normally left out due to the large technical problems involved in their computation. In the present work we found that the triple excitations make a substantial contribution (typically -0.5 to -1.0 a.u. in the static case) for OH as well as HF. Fortunately, this contribution tends to be cancelled by other double excitations which are also normally left out in numerical many-body computations.

Finally, it should be mentioned that types of V^{N-1} potentials other than that discussed so far were also investigated. In the case of OH a natural and physical choice would be to obtain the excited states in the field of the $^3\Sigma^-$ ground state of the OH^+ ion. This choice of single-particle potential actually led to excited-state orbital energies which were very close to those of the present V^{N-1} potential. The rate of convergence of the perturbation expansion based on the OH^+ potential was at best rather poor, and for the computation of $\alpha_\parallel(0)$ with the model Hamiltonian, there was actually no convergence at all through the lowest three orders.

C. Photoionization cross sections

Photoionization cross sections were calculated by inverting Eq. (13), as described in I and in Sec. II D. The isotropic polarizability

$$\alpha(i\eta)=\tfrac{1}{3}[2\alpha_\perp(i\eta)+\alpha_\parallel(i\eta)] \tag{19}$$

was computed for about 25 η values in the range $\eta=0$ to 12 a.u., and the discrete α values were fitted to a series of exponentials to obtain a continuous representation of $\alpha(i\eta)$. Basis functions were generated as described by Eqs. (14)–(16), and for OH a four-term expansion [cf. Eq. (14)] was found to be sufficient, with $k_0=2.60$ and $C=2.0$ [cf. Eq. (16)]. For HF the cross section $\sigma(\omega)$ extends to higher frequencies like the case for atomic neon, and five terms were necessary in the expansion, with $k_0=1.10$ and $C=2.0$. The numerical stability of the inversion procedure was checked by making reasonable changes of the parameters k_0 and C.

Computed cross sections are given in Tables IV and V for OH and HF, respectively, and computations were carried out for the two partitionings of the Hamiltonian and the two potentials V^N (Hartree-Fock) and V^{N-1}. The present way of computing the cross section yields a continuous curve for $\sigma(\omega)$, which is actually a measure for the total absorption coefficient and which should be zero for frequencies below the first excitation energy of the molecule. The photoionization cross section is certainly obtained only for frequencies above the ionization threshold.

The results obtained from the four different computations are all seen to be in reasonable agreement for OH as well as for HF. By the computation of the polarizabilities, it was concluded that the shifted Hamiltonian [cf. Eq. (8)] with the V^{N-1} potential tends to give the most reliable results. Hence, the cross sections obtained from this computation are shown in Figs. 2 and 3 for OH and HF, respectively.

TABLE IV. The cross section $\sigma(\omega)$ (Mb) as calculated from the inversion of Eq. (13) for OH. The total photoionization cross section is obtained for frequencies above the ionization threshold of $\omega_{th}=0.48$ a.u.

ω	Model Hamiltonian		Shifted Hamiltonian	
(a.u.)	V^N	V^{N-1}	V^N	V^{N-1}
0.00	0.00	0.00	0.00	0.00
0.30	1.91	2.91	2.96	2.47
0.40	6.67	8.06	7.73	7.29
0.50	11.18	12.70	12.03	11.77
0.60	14.33	15.70	14.85	14.80
0.70	16.01	17.03	16.16	16.31
0.80	16.51	17.09	16.32	16.64
0.90	16.23	16.35	15.75	16.19
1.00	15.49	15.19	14.76	15.31
1.10	14.51	13.86	13.59	14.21
1.30	12.31	11.21	11.20	11.87
1.50	10.18	8.92	9.05	9.69
1.70	8.26	7.04	7.22	7.79
2.00	5.83	4.85	5.03	5.46
2.50	3.00	2.45	2.56	2.79
3.00	1.40	1.14	1.19	1.30
3.50	0.60	0.49	0.51	0.56
4.00	0.25	0.20	0.21	0.23
5.00	0.04	0.03	0.03	0.03

TABLE V. The cross section $\sigma(\omega)$ (Mb) as calculated from the inversion of Eq. (13) for HF. $\sigma(\omega)$ represents the photoionization cross section for frequencies above the ionization threshold $\omega_{th}=0.59$ a.u.

ω	Model Hamiltonian		Shifted Hamiltonian	
(a.u.)	V^N	V^{N-1}	V^N	V^{N-1}
0.00	0.00	0.00	0.00	0.00
0.30	0.33	1.25	1.28	1.03
0.40	3.12	4.69	4.67	4.23
0.50	6.61	8.56	8.42	7.89
0.60	9.76	11.73	11.41	10.94
0.70	12.12	13.77	13.23	12.95
0.80	13.60	14.69	13.94	13.93
0.90	14.34	14.75	13.81	14.10
1.00	14.52	14.24	13.13	13.72
1.20	13.84	12.37	11.10	12.16
1.50	11.75	9.43	8.27	9.58
2.00	7.98	6.22	5.81	6.64
2.50	4.91	4.46	4.85	4.92
3.00	2.77	3.33	4.23	3.75
3.50	1.46	2.52	3.62	2.88
4.00	0.73	1.92	3.00	2.21
5.00	0.16	1.10	1.88	1.28
6.00	0.03	0.61	1.07	0.71
7.00	0.01	0.31	0.56	0.37
8.00	0.00	0.16	0.28	0.18
10.00	0.00	0.03	0.06	0.04

In Fig. 2 the present results are compared with the computed ones of Stephens and McKoy [7]. The results of Stephens and McKoy are based on numerical photoelectron continuum orbitals obtained using the iterative Schwinger variational technique and multiplet-specific Hartree-Fock orbitals. Thus, their computation does not go beyond the Hartree-Fock level of accuracy. The length-form results of Stephens and McKoy are shown in Fig. 2, since the present results were also obtained with the length form. As discussed in I, the velocity form is not relevant for the present method of computation.

From Fig. 2 it is clear that there are considerable discrepancies between the present results and those of Stephens and McKoy, both for the lowest- and for the highest frequencies. The velocity results of Stephens and McKoy which are not shown in Fig. 2 are, however, in

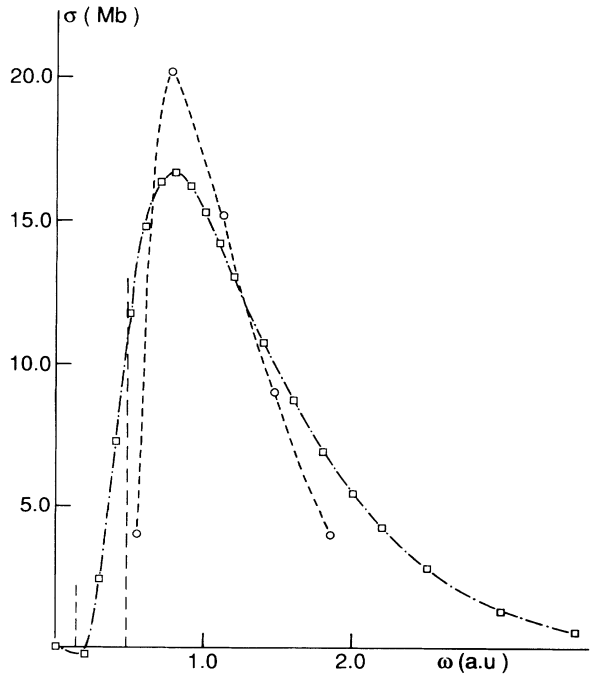

FIG. 2. Computed total absorption (photoionization) cross section for OH. □, present results; ○, Stephens and McKoy [7] (length form). The vertical dashed lines indicate the ionization threshold and the energy of the first excited $A^2\Sigma^+$ state, respectively.

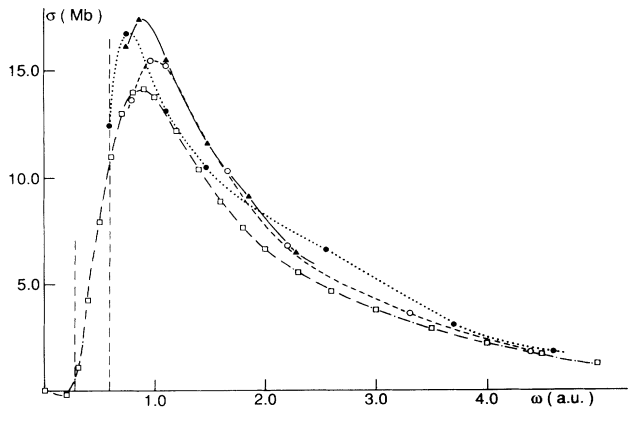

FIG. 3. Computed total absorption (photoionization) cross section for HF. □, present results; ○, Fægri and Kelly [5] (length form); ▲, Cacelli *et al.* [14] (length form); ●, experiment [35]. The vertical dashed lines indicate the ionization threshold and the onset of diffuse absorption bands [37], respectively.

somewhat better agreement with the present ones. Unfortunately, there seem to be no experimental results on OH so far.

In a similar way, Fig. 3 shows the present cross sections for HF compared with the computed ones of Fægri and Kelly [5] and Cacelli *et al.* [14]. The latter two computations are both on the Hartree-Fock level of accuracy. That of Fægri and Kelly is based on a single-center spherical wave approximation for the continuum orbitals, whereas that of Cacelli *et al.* is based on the Stieltjes technique, using a discrete basis set and single-center expansion. As for OH, the present cross sections for HF are seen to be lower than those obtained with single-center Hartree-Fock methods. It should, however, be mentioned that both Fægri and Kelly, Cacelli *et al.*, obtain velocity-form cross sections that are considerably lower than their length-form results, which are shown in Fig. 3.

Figure 3 also shows the experimental cross section of Carnovale *et al.* [35] obtained with the method of $(e,2e)$ spectroscopy. Except for frequencies closely above the ionization threshold, there is reasonable agreement between experiment and the three theoretical predictions shown in Fig. 3, including the present one. More experimental results obtained with different methods would certainly be of great interest for HF.

The real part of the polarizability on the real frequency axis as obtained from Eq. (17) and the computed cross section $\sigma(\omega)$ is shown in Figs. 4 and 5 for OH and HF, respectively. $\mathrm{Re}\alpha(\omega)$ yields information on the index of refraction $n(\omega)$ through the relation [36]

$$n(\omega)\approx 1+2\pi N\,\mathrm{Re}\alpha(\omega)\ , \tag{20}$$

where N is the number of molecules per unit volume. The energy of the first excited state is marked by the vertical dashed line in Figs. 4 and 5. For OH it is interesting to note that the maximum of $\mathrm{Re}\alpha(\omega)$ occurs at a frequency that is substantially higher (0.3 a.u.) than the frequency 0.15 a.u. corresponding to the first excited $A^2\Sigma^+$ state (configuration $\sigma\pi^4$). Hence, the $A^2\Sigma^+$ state seems to make a minor contribution to the polarizability of OH. This conclusion is also in agreement with the computed absorption cross section, which actually shows a small negative value at the excitation frequency of the $A^2\Sigma^+$ state (cf. Fig. 2).

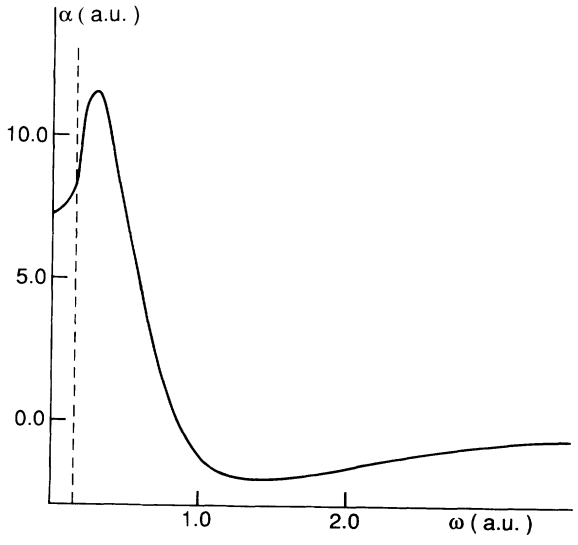

FIG. 4. Dispersion curve [real part of $\alpha(\omega)$ on the real frequency axis] for OH. The vertical dashed line indicates the energy of the first excited $A^2\Sigma^+$ state.

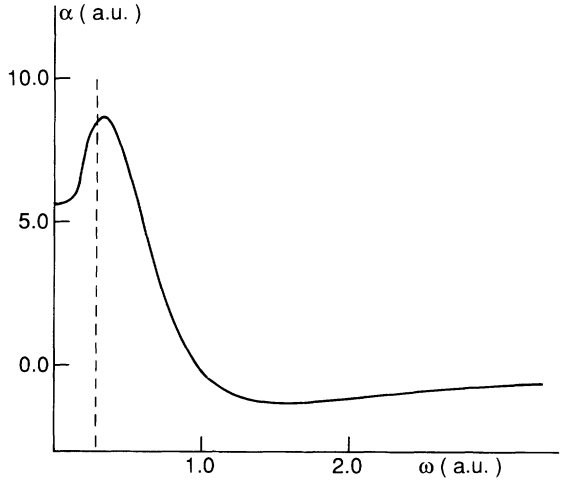

FIG. 5. Dispersion curve for HF. The vertical dashed line indicates the onset of diffuse absorption bands [37].

In HF, on the other hand, the maximum of $\mathrm{Re}\alpha(\omega)$ is found at a frequency very close to the frequency of 0.28 a.u. where the (continuous) absorption bands start [37]. Thus, in HF the first bound excited states seem to make a dominant contribution to the polarizability. Figure 5 also shows a small positive cross section at the lowest excitation energy in HF.

For OH as well as HF, the polarizability tends to obey the free-electron dispersion relation

$$\mathrm{Re}\alpha(\omega)\approx -\frac{n}{\omega^2} \tag{21}$$

for large frequencies, where n is the number of "free" electrons.

IV. CONCLUSION

The success of a method to compute atomic and molecular photoionization cross sections depends heavily on its ability to handle the many-body effects that play an essential role in the complex polarizability. In the present investigation a considerable effort has been put into the discussion of the rate of convergence of the many-body expansion. The choice of single-particle potentials for the excited states is in particular crucial. The potentials should be physical in the sense that they yield a fair description of the field felt by the outgoing electron. On the other hand, they have to be very carefully chosen to prevent the perturbation expansion from being divergent due to large interactions with the effective potential.

The molecular systems require the use of finite basis sets, and this allows less flexibility in the choice of

excited-state potentials than the numerical methods used for atomic systems. Compared with numerical work, the use of basis sets yields no explicit representation of the state of the free electron, and we have to carry the computation through for an N-particle system. Working with basis sets, the Hartree-Fock potentials are convenient in the sense that they will normally prevent divergencies of the perturbation expansion. They are, however, unphysical as the outgoing electron will feel the field of a neutral system. Hence, the Hartree-Fock potentials may yield slow convergence and poor results even when, as in the present case, the perturbation expansion is carried to the second order in the Coulomb interaction. In the present work this problem was solved by constructing single-particle potentials for the excited states that tend to minimize or eliminate the first-order contributions in the perturbation expansion.

The inversion of the integral equation [Eq. (13)] is another crucial point. Future work should probably be directed at working out methods of inversion that are more sophisticated than the present one. The present method of inversion should be quite adequate for frequency regions where the cross section is monotonically increasing of decreasing. Pronounced maxima or minima in the cross section will obviously be more difficult to describe, and narrow resonances will not be recovered at all since they make no contribution to Eq. (13).

ACKNOWLEDGMENTS

The present work was supported by the U.S. National Science Foundation and by the Norwegian Research Council for Sciences and the Humanities.

[1] M. Ya. Amusia and N. A. Cherepkov, Case Stud. At. Phys. **5**, 47 (1975).
[2] A. F. Starace, in *Corpuscles and Radiation in Matter I,* edited by W. Mehlhorn, Handbuch der Physik Vol. 31 (Springer, Berlin, 1980).
[3] H. P. Kelly, Phys. Scr. **T17**, 109 (1987).
[4] T. E. H. Walker and H. P. Kelly, Chem. Phys. Lett. **16**, 511 (1972).
[5] K. Fægri, Jr. and H. P. Kelly, Phys. Rev. A **23**, 52 (1981).
[6] R. R. Lucchese, G. Raseev, and V. McKoy, Phys. Rev. A **25**, 2572 (1982).
[7] J. A. Stephens and V. McKoy, J. Chem. Phys. **88**, 1737 (1988).
[8] M. T. Lee, J. A. Stephens, and V. McKoy, J. Chem. Phys. **92**, 536 (1990).
[9] L. Ackermann, A. Görling, and N. Rösch, J. Phys. B **23**, 2485 (1990).
[10] P. W. Langhoff and C. T. Corcoran, J. Chem. Phys. **61**, 146 (1974).
[11] P. W. Langhoff, C. T. Corcoran, J. S. Sims, F. Weinhold, and R. M. Glover, Phys. Rev. A **14**, 1042 (1976).
[12] J. T. Broad and W. P. Reinhardt, Chem. Phys. Lett. **37**, 212 (1976).
[13] T. N. Rescigno, C. F. Bender, B. V. McKoy, and P. W. Langhoff, J. Chem. Phys. **68**, 970 (1978).
[14] I. Cacelli, V. Carravetta, and R. Moccia, J. Phys. B **18**, 1375 (1985).
[15] I. Cacelli, V. Carravetta, and R. Moccia, Mol. Phys. **59**, 385 (1986).
[16] J. T. Broad and W. P. Reinhardt, J. Chem. Phys. **60**, 2182 (1974).
[17] T. N. Rescigno, C. W. McCurdy, Jr., and V. McKoy, Phys. Rev. A **9**, 2409 (1974).
[18] P. H. S. Martin, T. N. Rescigno, and V. McKoy, Chem. Phys. Lett. **29**, 496 (1974).
[19] S. Yabushita, C. W. McCurdy, and T. N. Rescigno, Phys. Rev. A **36**, 3146 (1987).
[20] L. Veseth, Phys. Rev. A **44**, 358 (1991).
[21] P. W. Atkins, *Molecular Quantum Mechanics* (Clarendon, Oxford, 1978), Part III.
[22] U. Fano and J. W. Cooper, Rev. Mod. Phys. **40**, 441 (1968).
[23] H. P. Kelly, Phys. Rev. **182**, 84 (1969).
[24] S. Wilson, *Electron Correlation in Molecules* (Clarendon, Oxford, 1984).
[25] L. Veseth, J. Phys. B **16**, 2891 (1983).
[26] I. Lindgren and J. Morrison, *Atomic Many-Body Theory* (Springer-Verlag, Berlin, 1982).
[27] Z. Qian, S. L. Carter, and H. P. Kelly, Phys. Rev. A **33**, 1751 (1986).
[28] J. D. Jackson, *Classical Electrodynamics,* 2nd ed. (Wiley, New York, 1975).
[29] D. M. Bishop and S. M. Cybulski, Mol. Phys. **71**, 667 (1990).
[30] L. Adamovicz, J. Chem. Phys. **89**, 6305 (1988).
[31] G. H. F. Diercksen, V. Kellö, and A. J. Sadley, Chem. Phys. Lett. **95**, 226 (1983).
[32] P. E. Cade and W. Huo, At. Data Nucl. Data Tables **12**, 415 (1973).
[33] H. Werner and W. Meyer, Mol. Phys. **31**, 855 (1976).
[34] J. S. Muenter, J. Chem. Phys. **56**, 5409 (1972).
[35] F. Carnovale, R. Tseng, and C. E. Brion, J. Phys. B **14**, 4771 (1981).
[36] N. Tralli, *Classical Electromagnetic Theory* (McGraw-Hill, New York, 1963).
[37] K. P. Huber and G. Herzberg, *Constants of Diatomic Molecules* (Van Nostrand, New York, 1979).